

Published in final edited form as:

Cancer Cell. 2012 September 11; 22(3): 304–317. doi:10.1016/j.ccr.2012.07.024.

EGF Receptor is Required for KRAS-induced Pancreatic Tumorigenesis

Christine M. Ardito^{1,*}, Barbara M. Grüner^{2,*}, Kenneth K. Takeuchi³, Clara Lubeseder-Martellato², Nicole Teichmann², Pawel K. Mazur⁴, Kathleen E. DelGiorno^{1,3}, Eileen S. Carpenter¹, Christopher J. Halbrook^{1,3}, Jason C. Hall^{1,3}, Debjani Pal¹, Thomas Briel², Alexander Herner², Marija Trajkovic-Arsic², Bence Sipos⁵, Geou-Yarh Liou³, Peter Storz³, Nicole R. Murray³, David W. Threadgill⁶, Maria Sibilina⁷, M. Kay Washington⁸, Carole L. Wilson⁹, Roland M. Schmid², Elaine W. Raines⁹, Howard C. Crawford^{1,3,10,**}, and Jens T. Siveke^{2,**}

¹Department of Pharmacological Sciences, Stony Brook University, Stony Brook, NY 11794

²II. Medizinische Klinik, Klinikum rechts der Isar, Technische Universität München, 81675 Munich, Germany

³Department of Cancer Biology, Mayo Clinic, Florida, Jacksonville, FL 32224

⁴Department of Genetics, Department of Pediatrics, Stanford University, Stanford, CA 94305

⁵Department of Pathology, University Hospital Tübingen, Tübingen, Germany

⁶Department of Genetics, North Carolina State University, Raleigh, NC, 27599

⁷Institute for Cancer Research, Department of Medicine I, Comprehensive Cancer Center, Medical University of Vienna, Vienna, Austria

⁸Department of Pathology, Vanderbilt University Medical Center, Nashville, TN, 37232

⁹Department of Pathology, University of Washington, Seattle WA, 98195

¹⁰Department of Research, Veterans Affairs Medical Center, Northport, NY 11768

SUMMARY

Initiation of pancreatic ductal adenocarcinoma (PDA) is definitively linked to activating mutations in the *KRAS* oncogene. However, PDA mouse models show that mutant *Kras* expression early in development gives rise to a normal pancreas, with tumors forming only after a long latency or pancreatitis induction. Here we show that oncogenic KRAS upregulates endogenous EGFR expression and activation, the latter being dependent upon the EGFR ligand sheddase, ADAM17. Genetic ablation or pharmacological inhibition of EGFR or ADAM17 effectively eliminates KRAS-driven tumorigenesis *in vivo*. Without EGFR activity, active RAS levels are not sufficient to induce robust MEK/ERK activity, a requirement for epithelial transformation.

© 2012 Elsevier Inc. All rights reserved.

**Correspondence: crawford.howard@mayo.edu (HCC); jens.siveke@lrz.tu-muenchen.de (JTS), listed alphabetically.

* contributed equally to this work, listed alphabetically

The authors have no conflicts of interest.

Publisher's Disclaimer: This is a PDF file of an unedited manuscript that has been accepted for publication. As a service to our customers we are providing this early version of the manuscript. The manuscript will undergo copyediting, typesetting, and review of the resulting proof before it is published in its final citable form. Please note that during the production process errors may be discovered which could affect the content, and all legal disclaimers that apply to the journal pertain.

INTRODUCTION

Pancreatic ductal adenocarcinoma (PDA) is almost universally fatal, but its remarkable genetic homogeneity has aided greatly in our understanding of its genesis and progression. Most PDA samples harbor oncogenic mutations in the *KRAS* gene, from early pancreatic intraepithelial neoplasia (PanIN) to PDA, marking mutant *KRAS* as the most prominent PDA initiating gene. Pancreas-specific mutant *Kras* expression in mice results in mouse PanIN (mPanIN) formation, eventually leading to PDA. Strikingly, even with universal expression of mutant *Kras* in early organogenesis, the pancreas develops normally, giving rise to a functional, tumor-free pancreas with preneoplastic lesions and mPanINs forming stochastically only after several weeks (Hingorani et al., 2003). Consistent with this, oncogenic *KRAS* mutations are found in human pancreata with no signs of PDA (Luttges et al., 1999). Together, these observations suggest that expression of mutant *Kras* requires ill-defined secondary events to initiate pancreatic tumorigenesis.

The ductal nature of PanIN and PDA suggests their derivation via transformation of normal duct epithelium or of progenitor cells capable of assuming a ductal morphology. Confounding this hypothesis, *Kras*^{G12D} expression directed to specific cellular compartments has shown that duct, islet and acinar cells can all give rise to mPanIN lesions (Gidekel Friedlander et al., 2009), but expression in the adult acinar or islet cell compartments requires pancreatitis induction (Carriere et al., 2009; Gidekel Friedlander et al., 2009; Guerra et al., 2007). This acquired sensitivity to transformation is attributed to acinar cell transdifferentiation to metaplastic ducts, which have progenitor-like characteristics (Miyamoto et al., 2003; Sharma et al., 1999) that may make them more susceptible to *KRAS*-induced oncogenesis. Consistent with this hypothesis, Hebrok and colleagues have shown that *KRAS*^{G12D} expression hijacks the regeneration process after tissue damage, promoting the metaplasia-to-PanIN transition (Morris et al., 2010).

Aberrant signal transduction pathways that control acinar-to-ductal metaplasia (ADM) are under intense study. Examination of chronic pancreatitis (CP) and PDA patient samples has shown an upregulation of epidermal growth factor receptor (EGFR, ERBB1) (Fjallskog et al., 2003; Korc et al., 1994; Tobita et al., 2003) and several of its ligands (Kobrin et al., 1994; Zhu et al., 2000). The relevance of this correlation is bolstered by the induction of metaplasia and desmoplasia *in vivo* by transgenic EGFR ligand overexpression (Means et al., 2003; Sandgren et al., 1990). *In vitro*, treatment of acinar cell explants with EGFR ligands, such as transforming growth factor alpha (TGFA), results in ADM (De Lisle and Logsdon, 1990; Means et al., 2005). Lineage tracing experiments confirm that metaplastic ducts arise in part from acinar cell transdifferentiation in response to tissue injury (Strobel et al., 2007), supporting a physiological relevance to acinar cell transdifferentiation. However, it is not known whether endogenous ligand activation of EGFR plays a role in ADM in pancreatic disease.

Taking advantage of the reproducible kinetics of tumor formation in PDA mouse models, we set out to address the contribution of EGFR activity to disease progression using genetic and pharmacological approaches.

RESULTS

EGFR Pathway Upregulation Precedes Tumorigenesis in *Kras*^{G12D} mice

EGFR is upregulated in PDA and PDA mouse models (Fjallskog et al., 2003; Korc et al., 1994; Tobita et al., 2003), Figure S1) though its function primarily has been associated with enhanced proliferation and invasiveness (Jaganathan et al., 2010; Larbouret et al., 2007; Pino et al., 2006; Zhao et al., 2010). To better dissect the role of EGFR in PDA progression,

we tested if EGFR was activated in the *Kras^{LSL-G12D/+};Ptf1a^{Cre/+}* mouse model (referred to henceforth as *Kras^{G12D}*), which reproducibly shows metaplasia and mPanIN formation beginning at ~8 weeks of age, with progression to PDA at ~1 year (Hingorani et al., 2003). Immunohistochemistry (IHC) for active EGFR (pY1068) was undetectable in wild-type pancreata, but easily detectable in acinar areas prior to mPanIN formation in 30 day old *Kras^{G12D}* mice and in mPanINs in 3 month old *Kras^{G12D}* mice (Figure 1A). To test if EGFR itself was upregulated, we analyzed mRNA isolated from 6 week old *Kras^{G12D}* pancreata by qRT-PCR, a time prior to significant metaplasia or neoplasia. Transcripts for both EGFR and TGFA, an EGFR ligand, were consistently upregulated ~2-fold (Figure 1B). Amphiregulin (AREG), another EGFR ligand, was also upregulated relative to wild-type controls, which had undetectable AREG levels (data not shown). Immunofluorescence staining (IF) for total EGFR showed upregulation in discrete acinar cell clusters in *Kras^{G12D}* pancreata (Figure 1C), becoming very prominent in larger acinar clusters, especially near areas of metaplasia and mPanIN, and was particularly high in metaplasia and mPanINs. Thus, EGFR pathway upregulation is a very early event in pancreatic tumorigenesis. Moreover, the stochasticity of EGFR overexpression in acini prior to mPanIN formation was reflected the pattern of tumor formation, suggesting a role for EGFR signaling in transformation of the acinar cell compartment.

To test if acinar cell EGFR activation coincided with ductal transdifferentiation, we examined primary acinar cell explants isolated from *Kras^{G12D}* mice, which spontaneously transdifferentiate into duct cells when embedded in fibrillar collagen. On day 1 of culture, active pY1068 EGFR was undetectable (Figure 1D), but was strongly positive by day 3, as transdifferentiation took place. Activation correlated with increased EGFR expression, as determined by qRT-PCR (Figure 1E). Thus, EGFR upregulation and activation is initiated by KRAS *in vitro* and *in vivo* in a manner consistent with its involvement in preneoplastic duct formation.

Inhibition of EGFR limits pancreatic tumorigenesis but not progression

To test if EGFR activity is required for pancreatic preneoplastic lesion formation, we examined the effects of pharmacological EGFR inhibition in a highly aggressive PDA model. *Kras^{LSL-G12D/+};Ptf1a^{Cre/+};Trp53^{fl/fl}* mice, referred to as *Kras^{G12D};p53^{KO}*, develop invasive PDA at 4–6 weeks of age (Bardeesy et al., 2006). Starting at 1 week of age, *Kras^{G12D};p53^{KO}* mice were treated daily with either cetuximab, a monoclonal antibody that blocks ligand interaction with the receptor; erlotinib, a small molecule EGFR tyrosine kinase inhibitor; or vehicle for 3 weeks. Histological examination showed substantial areas of normal, non-transformed tissue with either treatment, and a significantly reduced number of CK19⁺ ductal lesions compared to control (Figure 2A–C).

Retention of substantial areas of normal tissue with EGFR inhibition supported a role for EGFR signaling in tumor initiation. To test this possibility definitively, we mated *Kras^{G12D};p53^{KO}* mice with conditional *Egfr* knockout mice (Lee and Threadgill, 2009; Natarajan et al., 2007). Mice with EGFR ablated from the pancreas (*Egfr^{fl/fl};Ptf1a^{Cre/+}*, referred to as *Egfr^{KO}*) were viable and showed no gross pancreatic abnormalities. Consistent with the inhibitor experiments, *Kras^{G12D};p53^{KO};Egfr^{KO}* pancreata retained substantial areas of normal acinar tissue, whereas age-matched *Kras^{G12D};p53^{KO}* pancreata were completely replaced by tumorous tissue (Figure 2D&E). IHC for EGFR confirmed that ~50% of mPanINs that formed in these mice were EGFR negative (Figure S2A), with the other half likely a product of incomplete recombination of the *Egfr* locus. To gain insight into the escape from EGFR dependency, we established cell lines from *Kras^{G12D};p53^{KO};Egfr^{KO}* pancreata. Confirming EGFR loss by western blot, we assessed other signaling and differentiation changes compared to EGFR wild-type controls. Two pathways in particular showed consistent upregulation and activation in the absence of

EGFR: the Notch pathway and MET, both of which have been implicated in pancreatic tumor progression (Figure S2B), most notably in the ADM process (Means et al., 2005; Miyamoto et al., 2003).

EGFR inhibition has been shown to be minimally effective in PDA patients. To test if the *Kras*^{G12D};*p53*^{KO} model reflected the clinical data, we treated mice with MRI-detectable advanced PDA with gemcitabine or erlotinib plus gemcitabine. Combination-treated mice showed no significant difference in lifespan compared to gemcitabine treatment alone (Figure 2F) and showed no reduction in tumor burden by MRI, consistent with independence from EGFR after progression to PDA.

EGFR inhibition most clearly affected pancreatic tumorigenesis, leading us to explore its effects more thoroughly in the slower-progressing *Kras*^{LSL-G12D/+} model. Tumor burden of *Kras*^{G12D} and *Egfr* knockout *Kras*^{G12D} mice (*Kras*^{G12D};*Egfr*^{KO}) was assessed at various ages by relative pancreatic mass, histology, loss of normal acinar (amylase⁺) tissue and appearance of MUC5AC⁺ ductal lesions (Figures 3A–C and S3A&B). By all criteria, *Egfr* ablation almost completely blocked tumorigenesis. Unlike *Kras*^{G12D};*p53*^{KO};*Egfr*^{KO} mice, all metaplasia and mPanIN that formed in *Kras*^{G12D};*Egfr*^{KO} mice were EGFR positive (Figure S3D), suggesting incomplete recombination of the *Egfr* locus and reinforcing the need for EGFR in tumorigenesis. These data also suggested that p53 inactivation itself allows for escape from EGFR dependency. The tumorigenesis block was not due to a failure to recombine the silenced *Kras*^{G12D} allele (Figure S3E).

Coordinated upregulation of *Tgfa*, *Areg* and *Egfr* in *Kras*^{G12D} pancreata, together with the effectiveness of cetuximab, suggested that receptor ligation is a necessary step in pancreatic tumorigenesis. EGFR ligands are generally shed from the cell surface by metalloproteinase “shedases”, but can also activate receptor in their membrane-bound forms in a juxtacrine manner (Singh and Harris, 2005). TGFA and AREG share a common primary shedase in ADAM17 (Sahin et al., 2004). To test if EGFR ligand shedding was necessary for tumorigenesis, we crossed a conditional *Adam17* knockout mouse line (*Adam17*^{ΔEx5/ΔEx5}) into the *Kras*^{G12D} background (*Kras*^{G12D};*Adam17*^{KO}). Pancreas-specific *Adam17* knockout mice (*Adam17*^{ΔEx5/ΔEx5};*Ptf1a*^{Cre/+}, referred to as *Adam17*^{KO}) were viable and showed no gross pancreatic abnormalities. To assess tumor formation in the *Kras*^{G12D};*Adam17*^{KO} background, we aged mice and examined their pancreata for tumor development. Indeed, *Kras*^{G12D};*Adam17*^{KO} mice phenocopied *Kras*^{G12D};*Egfr*^{KO} mice, showing a similar degree of protection from tumorigenesis (Figures 3A–C and S3A&C), with no effect on *Kras*^{G12D} recombination (Figure S3E). These results are consistent with EGFR activation by ADAM17-dependent ligand shedding being a necessary step in KRAS-driven pancreatic tumorigenesis.

Pancreatitis-associated Tumorigenesis Requires EGFR and ADAM17

Oncogenic *Kras* expression confined to acinar or islet cell compartments, requires pancreatitis for PDA formation (Gidekel Friedlander et al., 2009; Guerra et al., 2007). EGFR overexpression in *Kras*^{G12D} acinar cells suggested that EGFR ablation blocks transformation of this cellular compartment. To test if EGFR activity is required for pancreatitis-dependent, acinar cell-derived tumorigenesis, we treated 30 day old *Kras*^{G12D}, *Kras*^{G12D};*Egfr*^{KO} and *Kras*^{G12D};*Adam17*^{KO} mice with 250 μg/kg cerulein, a known inducer of pancreatic damage, daily for 5 days, followed by 7 days recovery. With cerulein treatment, *Kras*^{G12D} mice showed an almost complete replacement of normal pancreatic tissue with fibrotic, inflamed tissue and the majority of epithelia replaced by metaplasia and mPanIN. Both *Kras*^{G12D};*Egfr*^{KO} and *Kras*^{G12D};*Adam17*^{KO} mice were almost completely protected from this dramatic transition (Figure 3D–G).

Noting the earlier correlation between the patterns of EGFR overexpression and spontaneous tumor formation, we tested if cerulein treatment affected EGFR expression. Using a truncated cerulein treatment protocol (Figure 3H), we examined EGFR expression prior to rampant epithelial morphogenesis (Figure 3I). In 34 day old saline-treated controls, EGFR was minimally expressed in wild-type pancreata. As noted previously, in *Kras^{G12D}* controls, EGFR was elevated in discrete acinar clusters (1.3% of acinar cells). In contrast, 3 days of cerulein treatment in wild-type mice induced EGFR in discrete acini (<1% of total) after 1 day recovery, which returned to baseline levels with 3 days recovery. Strikingly, cerulein treatment of *Kras^{G12D}* mice induced very high EGFR expression in 73% of acinar cells with one day recovery, which was sustained after 3 days recovery and elevated further in metaplasia that had begun to form. Once again, EGFR overexpression in acinar cells reflected the pattern of the eventual tumor formation in this model.

The striking upregulation of EGFR in acinar cells suggested that this cellular compartment is prominently affected by its activity. Besides inducing acinar cell transdifferentiation, EGFR is known to both protect cells from apoptotic cell death and to induce proliferation. Cleaved caspase-3 IHC showed no significant upregulation of apoptosis in 6 week old *Kras^{G12D}* pancreata (data not shown). In contrast, proliferation, as measured by BrdU incorporation, increased ~4 fold in *Kras^{G12D}* acinar cells compared to wild-type, with this increase reduced by half in *Kras^{G12D};Egfr^{KO}* acinar cells (Figure 3J&K). This difference was exaggerated in cerulein-treated mice, where >10% of acinar cells in *Kras^{G12D}* mice incorporated BrdU, with no increase under the same conditions in *Kras^{G12D};Egfr^{KO}* pancreata. Consistent with this, CyclinD1 was upregulated in acinar cells of *Kras^{G12D}* and cerulein-treated *Kras^{G12D}* mice, but remained unchanged in *Kras^{G12D};Egfr^{KO}* pancreata with or without cerulein (Figure 3L&M).

EGFR activity is required for metaplastic duct formation

The dependency of acinar cell derived pancreatic tumorigenesis on pancreatitis has been attributed to the need for ADM prior to transformation (Gidekel Friedlander et al., 2009). Chronic activation of EGFR is sufficient to induce ADM *in vitro* (De Lisle and Logsdon, 1990) and *in vivo* (Sandgren et al., 1990). To test if EGFR signaling is necessary for this process, we employed several *in vivo* and *in vitro* models of ADM. Chronic overexpression of the EGFR ligand TGFA in the *Ela-Tgfa* transgenic model induces substantial ductal metaplasia and fibrosis after several weeks of transgene expression (Sandgren et al., 1990). Ablation of either *Egfr* or *Adam17* effectively eliminated TGFA-induced metaplasia *in vivo* even at one year of age (Figure S3F), reinforcing the necessity for ligand shedding in the ADM process.

Turning to metaplasia associated with experimental pancreatitis, we employed a cerulein treatment protocol that produced a chronic-pancreatitis-like phenotype in wild-type mice, marked by replacement of acinar tissue with metaplastic ducts and a reactive and inflamed stroma (Figure S3G). Both *Egfr^{KO}* and *Adam17^{KO}* mice were strongly protected from most aspects of pancreatitis, including ADM and the parallel stromal response. Quantitation of inflammatory cell infiltration into the damaged tissue confirmed a significant loss of this response (Figure S3H&I). Protein arrays revealed that several cytokines were significantly lower in cerulein treated *Egfr^{KO}* pancreata compared to wild-type, including RANTES, IL16, CXCL13 and IL23 (data not shown). However, the common expression of each of these factors by reactive inflammatory and other stromal cells suggested that these lower levels were possibly a secondary effect of the reduction in inflammatory infiltrates. Two pro-inflammatory proteins that were definitively produced by the metaplastic epithelia, as well as the stroma, were COX-1 and COX-2 (Figure S3J), suggesting that the inability of *Egfr^{KO}* pancreata to form metaplastic ducts contributes to the reduced inflammatory response.

The block in the pancreatitis phenotype was not due to gross loss of cerulein-induced signal transduction. When treated with cerulein to induce acute pancreatitis, mice of all genotypes showed a gain of pancreatic wet weight associated with edema, increased serum amylase levels, areas of tissue necrosis and induction of acinar cell SOX9 expression (Figure S3K–N).

We then tested if *in vitro* ADM required EGFR activation. *In vitro* ADM in collagen-embedded acinar cell explants is usually induced by addition of ectopic EGFR ligand. To more closely simulate the *in vivo* animal models, and to bypass direct EGFR stimulation, we chose to induce *in vitro* ADM either by expression of *Kras*^{G12D} or by addition of low concentrations of cerulein into the culture medium.

Acinar cell explants derived from *Kras*^{G12D} mice transdifferentiated spontaneously in culture within 3 days, as determined by coimmunofluorescence for the acinar and duct cell markers, amylase and CK19, respectively. This transition was almost entirely absent in explants derived from *Kras*^{G12D};*Egfr*^{KO} mice (Figure 4A&B), arresting at a nestin-positive intermediate stage (Miyamoto et al., 2003); Figure S4A&B).

We found also that treatment of wild-type acinar cell explants with cerulein induced ADM within 5 days (Figure 4C). Both *Egfr*^{KO} and *Adam17*^{KO} explants were strongly resistant to this effect, although *Egfr*^{KO} explants were more so (Figure 4C&D), indicating possible compensation from other sheddases. Like KRAS^{G12D} (Figure 1C), cerulein also induced EGFR activation, in an ADAM17 dependent manner (Figure S4C). We then examined expression of the EGFR ligands and ADAM17 substrates TGFA and AREG in acinar explants. While AREG was not detected (data not shown), TGFA was induced by the third day of cerulein treatment (Figure S4D), independent of genotype, confirming that the mutant acinar cells remain cerulein responsive. Finally, because ADAM17 is known to shed several bioactive cell surface molecules, we confirmed that the *Adam17*^{KO} ADM blockade did not require shedding of other substrates by rescuing the wild-type phenotype with addition of TGFA to the culture medium (Figure S4E).

The dependency of pancreatitis-associated and *in vitro* ADM upon acinar cell EGFR and ADAM17 led us to test the relevance of these findings to human disease. Expression of components of the EGFR pathway in human CP, including active EGFR (pY1068), ADAM17 and TGFA and AREG was determined by IHC (Figure S4F). Regardless of CP type (alcoholic, familial or spontaneous), active EGFR, ADAM17 and TGFA were consistently upregulated, particularly in acinar cells adjacent to inflamed and fibrotic stroma in 10/10 CP samples. AREG was consistently expressed in ductal metaplasia adjacent to non-expressing acinar cells. Thus, activation of the EGFR circuitry *in vivo* and *in vitro* is reflected in human CP.

EGFR-dependent ERK activation is Required for Pancreatic Tumorigenesis

Initially, we hypothesized that EGFR was responsible for activation of some of the pathways that have been shown to be important for pancreatic tumorigenesis, including STAT3 and RAC1. Contrary to these possibilities, we observed substantial pSTAT3 in *Kras*^{G12D};*Egfr*^{KO} pancreata comparable to *Kras*^{G12D} tissue (Figure S5A). We also saw no change in active RAC pull-down experiments (data not shown). Recent data suggesting that RAS activation must reach a minimum threshold in order to transform the pancreas (Ji et al., 2009) led us to examine if EGFR and ADAM17 inhibition or ablation is consistent with this model by examining downstream effectors of RAS, including PI3K/AKT (pAKT) and MAPK (pERK1/2). *Kras*^{G12D};*Egfr*^{KO} mice showed no diminution of active AKT compared to control *Kras*^{G12D} mice (Figure 5A), suggesting no difference in PI3K activity. In contrast, we observed ~2-fold lower levels of pERK in 3 month old *Kras*^{G12D};*Egfr*^{KO} pancreatic

lysates (Figure 5A). Since this difference may be an indirect effect of enhanced pERK levels in tumors that form only in *Kras*^{G12D} controls, we confirmed a similar loss of pERK in 4 week old pancreatic lysates, prior to substantial transformation (Figure 5A, lower panel). IHC for pERK in 4 week old *Kras*^{G12D} mice revealed several positive isolated acinar regions (0.8% of total), whereas in *Kras*^{G12D};*Egfr*^{KO} mice, pERK was limited to stromal cells (Figure 5B). ERK activation was also clearly detectable in 88% of acinar cell clusters in wild-type cerulein-treated acinar explants, compared to 4.2% and 10.8% in *Egfr*^{KO} and *Adam17*^{KO} explants, respectively (Figure 5C).

KRAS oncogenic mutations are dominant, usually only affecting a single allele. Thus, approximately half the KRAS protein expressed is wild-type and turns over GTP at a rapid rate thus inactivating signaling. Active EGFR is known to relocalize wild-type KRAS to the plasma membrane via Grb2/Sos where it is activated (Basu et al., 1994; Gale et al., 1993). Consistent with this, co-immunoprecipitation and co-immunofluorescence experiments showed clear interaction and colocalization of KRAS and EGFR in *Kras*^{G12D} expressing tumor cell lines and acinar explants (Figure S5B&C). Using isolated acinar cells from WT, *Kras*^{G12D}, *Kras*^{G12D};*Egfr*^{KO} and *Kras*^{G12D};*ADAM17*^{KO} mice, we found an upregulation of both total and active RAS in *Kras*^{G12D} acinar cells (Figure 5D), consistent with previous reports (Ji et al., 2009). However, in *Kras*^{G12D};*Egfr*^{KO} and *Kras*^{G12D};*ADAM17*^{KO} cells, active RAS was reduced by more than 50%, while the upregulation of total RAS remained, leaving the active/total RAS ratios an average of 55% and 45% lower than *Kras*^{G12D} cells, respectively.

We next tested if EGFR activity was required for maintenance of ERK activity when *Kras* is mutated. Treatment of isolated *Kras*^{G12D} acinar cells with erlotinib reduced the active RAS/total RAS ratio by an average of 39.8% compared to control, with no effect on total RAS expression (Figure 5E). We then treated *Kras*^{G12D} mice with cerulein to induce rampant transformation (Figure 3D) then treated acutely with erlotinib by oral gavage 12, 6 and 2 hours prior to tissue harvest. Compared to vehicle, erlotinib treatment reduced pERK levels by an average of 46% (Figure 5F). Treated pancreata showed an obvious reduction of pERK IHC, especially in isolated mPanINs (Figure 5G). Unlike our observations in *Egfr*^{KO} mice, acute erlotinib treatment dramatically reduced pAKT staining in mPanINs (Figure 5G), suggesting an acute effect on PI3K signaling that is apparently compensated for under conditions of chronic inhibition. Consistent with the knockout mice, no alteration in pSTAT3 was observed (Figure 5G). Erlotinib-treated pancreata also showed a dramatic ~4-fold upregulation of cleaved caspase-3 IHC positive cells (Figure 5H) and a significant decrease in CyclinD1 expression (Figure 5I), indicating that EGFR activity is critical for survival and proliferation of metaplastic and mPanIN epithelia. EGFR dependency is also demonstrable in human PDA cell lines, with both RAS and ERK activity responsive to EGFR inhibition and activation, even in *KRAS* mutant cells (Figure S5D). We also found upregulation of pERK IHC in acinar cells of human CP samples (Figure S5E), consistent with a role in ADM in human disease.

We have shown that EGFR is required for ADM and ERK activation and that EGFR and pERK are upregulated in acinar cells in human CP. To test if ERK activation is involved in ADM *in vitro* and pancreatic tumorigenesis *in vivo*, we employed the allosteric MEK1/2 inhibitor BAY 86-9766 (Iverson et al., 2009). BAY 86-9766 treatment of *Kras*^{G12D} acinar explants strongly blocked transdifferentiation (Figure 6A&B). We then treated 6-week old *Kras*^{G12D} mice with cerulein to induce pancreatitis. Concomitant with pancreatitis induction and continuing for 3 weeks after, mice were treated daily with 25 mg/kg BAY86-9766 or vehicle by oral gavage (Figure 6C). As expected, pERK levels in BAY86-9766-treated pancreata were reduced (Figure 6D) and vehicle-treated *Kras*^{G12D} mice developed fibrotic, inflamed tissue with the majority of epithelia replaced by metaplasia and mPanIN. In

contrast, BAY86-9766-treated mice retained mostly phenotypically normal tissue with only rare MUC5AC⁺ mPanINs (Figure 6E&F).

DISCUSSION

The reproducible tumor onset and progression in the *Kras*^{G12D} PDA model has allowed us to explore how EGFR affects the transition of normal epithelia to neoplastic lesions. We find that KRAS upregulates EGFR in distinct, phenotypically normal acinar clusters prior to formation of metaplasia and mPanINs. Acinar cell upregulation of EGFR is rapid in cerulein-induced pancreatitis, with KRAS^{G12D} activity able to sustain the elevated expression. Most importantly, blocking EGFR activity effectively eliminates KRAS-initiated pancreatic tumorigenesis, with or without pancreatitis induction, due to its critical role in amplifying ERK activation within the pancreas. Further, EGFR is critical for acinar cell proliferation and its stimulation of MEK is necessary for transdifferentiation of transformation-resistant acinar cells to a transformation-sensitive, progenitor cell-like, metaplastic duct cell. Thus, we propose that EGFR's major role in pancreatic tumorigenesis lies in its control of the differentiation of neoplastic precursors and, after tumor initiation, maintenance of ERK activity.

EGFR has been implicated in the pathogenesis of several epithelial cancers (Normanno et al., 2006). Inappropriate EGFR activation results from mutation of the receptor or overexpression of its ligands and their ADAM sheddases. Its contributions in *RAS*-mutated tumors are presumed to be through activation of complementary oncogenic pathways, as its abilities to activate the RAS pathway would be redundant. Nonetheless, upregulation of EGFR, its ligands and ADAM17 have been reported in PDA (Friess et al., 1996; Ringel et al., 2006), consistent with their importance in these usually *Kras*-mutant cancers. Several studies show that constitutive RAS signaling is not sufficient to compensate for EGFR activity. EGFR is necessary for growth (Dlugosz et al., 1997) and survival (Sibilia et al., 2000) of RAS-initiated cutaneous squamous cell carcinoma and maintains the stem-cell like nature of transformed keratinocytes (Hansen et al., 2000). In H-RAS initiated melanoma, an EGFR autocrine loop is required for tumor cell maintenance and survival (Bardeesy et al., 2005). In PDA cell lines, the unique activities of EGFR promote cell proliferation and invasion even when *KRAS* is mutated (Jaganathan et al., 2010; Larbouret et al., 2007; Pino et al., 2006; Zhao et al., 2010). Overall, the majority of studies support models where EGFR in *RAS*-mutated tumors is generally involved in post-transformation functions. Two studies provide notable exceptions where, *in vitro*, RAS transformation of otherwise normal immortalized cells requires EGFR activity (Gangarosa et al., 1997; Sibilia et al., 2000). In addition, concomitant pancreatic activation of oncogenic KRAS and EGFR signaling leads to accelerated formation of high-grade preneoplastic lesions and PDA, (Siveke et al., 2007). Our data support a model where endogenous EGFR signaling is required to maintain the critical threshold of RAS activity required for tumorigenesis (Ji et al., 2009). Based on numerous experimental approaches, loss of EGFR signaling resulted in a ~ 50% drop in active RAS, consistent with continual stimulation of GTP loading of the highly catalytically active wild-type RAS proteins, though we cannot eliminate the possibility that it is required for the occasional reactivation of the catalytically-impaired mutant KRAS.

Much has been made recently of experimental pancreatitis being required for transformation of oncogenic KRAS expressing acinar cells (Carriere et al., 2009; Gidekel Friedlander et al., 2009; Guerra et al., 2011; Guerra et al., 2007). In this model, cerulein induces intracellular activation of digestive enzymes, leading to cellular stress and necrosis. Necrosis attracts inflammatory cells, which cooperate with oncogenic KRAS in the epithelia to induce tumor formation by overcoming cellular senescence (Guerra et al., 2011; Lee and Bar-Sagi, 2010). While this provides a satisfying connection between PDA and one of its primary risk factors,

our data show that KRAS and cerulein induce transdifferentiation of acinar cells *in vitro* by inducing EGFR expression and ADAM17-dependent activation, demonstrating that the earliest steps in this program are initiated cell-autonomously. Even so, since parenchymal EGFR ablation also dampens the stromal response, definitive separation of epithelial and stromal contributions to tumorigenesis is complicated. EGFR is known to influence the expression of inflammatory cytokines (Mascia et al., 2010; Monick et al., 2005) and expression of the proinflammatory COX proteins in metaplastic ducts suggests that reactive epithelia promote the host response. Unlike EGFR or pERK activity, however, we do not find COX upregulation in acinar cells, suggesting this is not direct control of gene expression by EGFR signaling, but is inherent to the metaplastic duct phenotype.

The role of EGFR as a therapeutic target in PDA is complex. In unselected metastatic PDA patients, anti-EGFR therapy has only a modest survival effect, however subgroups of patients and defined molecular subtypes respond to EGFR targeting (Collisson et al., 2011; Jimeno et al., 2008; Moore et al., 2007). In our study, EGFR-negative PDA developed in *Kras^{G12D};p53^{KO};Egfr^{KO}* mice, albeit with reduced efficiency. In addition, *Kras^{G12D};p53^{KO}* mice showed no additional survival advantage with erlotinib treatment, indicating that development and progression to PDA can be EGFR independent in a p53-null setting. While we have some indication of what may be compensating for EGFR loss, such as MET activation, this activity was detectable in only a minority of EGFR negative tumors, possibly suggesting multiple routes for bypassing EGFR deficiency. Defining the underlying molecular cues and the role of p53 inactivation as a potential contraindication of responsiveness to EGFR inhibition are important issues to be resolved.

In summary, we have identified a critical role for EGFR in KRAS' reprogramming of the pancreatic epithelia *en route* to tumorigenesis. EGFR activation in this context requires ADAM17 and results in a substantial amplification of MEK signaling. The ADAM17/EGFR/MEK signaling axis is critical for some of the fundamental pathologies associated with PDA risk, such as formation of metaplastic ducts in pancreatitis, suggesting that there may be benefit in targeting the pathway in these at-risk patients, to restore homeostasis and thereby reduce the chance of tumorigenesis.

EXPERIMENTAL PROCEDURES

Mice

Kras^{LSL-G12D/+}, Ptf1a^{Cre/+}, Ela-Tgfa, Trp53^{fl/fl}, Adam17^{ΔEx5/ΔEx5} and *Egfr^{fl/fl}* strains have been described previously (Hingorani et al., 2003; Kawaguchi et al., 2002; Lee and Threadgill, 2009; Marino et al., 2000; Natarajan et al., 2007; Sandgren et al., 1990; Siveke et al., 2007; Tang et al., 2011). Experiments were conducted in accordance with the Office of Laboratory Animal Welfare, the German Federal Animal Protection Laws and approved by the Institutional Animal Care and Use Committees at the Technical University of Munich, Stony Brook University and Mayo Clinic.

Histology, IHC, IF and Western Blot

Distribution and use of all human samples was approved by the Institutional Review Boards of Vanderbilt University Medical Center and the Mayo Clinic. IHC was performed on a Ventana XT (Tuscon, AZ) autostainer or as previously described (Siveke et al., 2007). For total EGFR and phospho-ERK IHC, mice were anesthetized and perfused with 4% paraformaldehyde. All IHC was counterstained with hematoxylin except amylase/CK19 dual IHC. Quantitation of amylase positive area was performed on singly DAB stained sections using Olympus cellSens Dimension software. Quantitation represents the average of 15–20 20X fields of view from 3 mice of each genotype, treatment regimen or time point, as

indicated. IF and western blot were performed according to standard protocols (Siveke et al., 2007). Confocal IF images were collected on a Leica SP2 or a Ziess-LSM-510 Meta confocal microscope at consistent gain and offset. Antibodies are in Supplemental Information.

RAS activity assay

GST-Raf-1-RBD fusion protein was prepared by modifying procedures published elsewhere (Castro et al., 2005). Details of cell preparation and protocol modifications are found in Supplemental Information.

Quantitative RT-PCR

Real-Time PCR was performed as previously described (Siveke et al., 2007). For protocol details, see Supplemental Information.

Preparation of Pancreatic Epithelial Explants Culture

Pancreatic epithelial explants were as described previously (Heid et al., 2011). Either recombinant human TGF- α (rh TGF α , R&D Systems, final concentration 50 ng/ml) or cerulein (American Peptide Company, Sunnyvale, CA, 2.6 pM final concentration) were added as indicated. For MEK inhibition, BAY 86-9766 (provided by Bayer Schering) was added at indicated concentrations.

For each genotype, experiments with acinar epithelial explants were performed with the following numbers of mice: *WT* n=15, *Egfr*^{KO} n=5, *Adam17*^{KO} n=10, *Kras*^{G12D} n=7, *Kras*^{G12D}; *Egfr*^{KO} n=10. *WT* plus BAY 86-9766 n=3, *Kras*^{G12D} plus BAY 86-9766 n=3. For quantification, acinar explants were seeded in triplicate and cell clusters were counted from at least 3 optical fields/well.

Cerulein treatments

To induce a CP-like phenotype, 250 μ g/kg twice daily injections of cerulein were administered i.p. for three weeks, with 24 hr recovery. *Kras*^{G12D} and knockout derivatives were treated with 250 μ g/kg cerulein once daily for 5 consecutive days and allowed to recover for 1 wk before tissue harvesting. For examining EGFR protein induction, 1 daily 250 μ g/kg i.p. dose was administered for 3 days and allowed to recover for 1 or 3 days, as indicated.

In vivo inhibition of MEK in pancreatitis-induced tumors

6 week old *Kras*^{G12D} mice were treated to induce pancreatitis, as described previously (Morris et al., 2010). On day 1 post cerulein injection, mice received a single daily dose of 25 mg/kg BAY 86-9766 or vehicle by oral gavage, 6 days per week for three weeks.

In vivo treatment of *Kras*^{G12D}; *p53*^{KO} mice with erlotinib or cetuximab

7 day old *Kras*^{G12D}; *p53*^{KO} mice were injected i.p. with either cetuximab (twice per week, 2 mg/kg), erlotinib (daily, 25 mg/kg) or vehicle (daily) for three weeks and sacrificed at 28 days of age. To assess efficacy of gemcitabine alone and in combination with erlotinib, mice with detectable tumor burden by MRI, determined by a clinical 1.5T MRI device, were treated daily with gemcitabine i.p. (120 mg/kg, 4 doses every third day) or gemcitabine i.p. (100 mg/kg, 4 doses every third day) in combination with erlotinib (daily, 50 mg/kg) by oral gavage. Tumor burden was monitored by MRI. For acute erlotinib treatment, *Kras*^{G12D} were treated with 5 daily doses of 250 μ g/kg cerulein, allowed to recover for 1 week and then treated with 100 mg/kg erlotinib 12, 6 and 2 hrs before sacrifice and tissue harvest.

Statistical analysis

Statistical analyses were performed using the Mann-Whitney-test for non-normally distributed, unpaired data. Tumor burden was compared between strains using one-way ANOVA. With all box plots, the bottom and top of the box are the 25th and 75th percentile and the central line is the median of the data. The whiskers represent maximum and minimum values, with the remaining dots being outliers.

Supplementary Material

Refer to Web version on PubMed Central for supplementary material.

Acknowledgments

This work was supported by a VA Merit Award, the Knapp Chair for Pancreatic Cancer Research and NIH grants R01CA129579 and R03CA129579 to HCC; NIH grants P01HL018645 and R01HL067267 to EWR; a pilot and feasibility award from University of Washington Nutrition and Obesity Center grant DK035816 to CLW; FWF (W1212), the EC (LSHC-CT-2006-037731) and the GEN-AU program “Austromouse” (GZ200.147/1-VI/1a/2006 and 820966) to MS; R01CA092479 and P50CA106991 to DWT; R01CA140290 to NRM; R01CA140182 to PS; by P50CA095103 for the Vanderbilt University Medical Center GI Spore Tissue Core; by Deutsche Krebshilfe (Grant 109992 to JTS.); by the German Federal Ministry of Education and Research (National Genomic Research Network (NGFN-Plus), 01GS08115 to JTS and RMS); by the German Research Foundation (SFB824/C4 to JTS). TROMAIII antibody, developed by Rolf Kemmler, was obtained from the Developmental Studies Hybridoma Bank developed under the auspices of the NICHD and maintained by The University of Iowa, Department of Biology, Iowa City, IA 52242.

References

- Bardeesy N, Aguirre AJ, Chu GC, Cheng KH, Lopez LV, Hezel AF, Feng B, Brennan C, Weissleder R, Mahmood U, et al. Both p16(Ink4a) and the p19(Arf)-p53 pathway constrain progression of pancreatic adenocarcinoma in the mouse. *Proc Natl Acad Sci U S A*. 2006; 103:5947–5952. [PubMed: 16585505]
- Bardeesy N, Kim M, Xu J, Kim RS, Shen Q, Bosenberg MW, Wong WH, Chin L. Role of epidermal growth factor receptor signaling in RAS-driven melanoma. *Mol Cell Biol*. 2005; 25:4176–4188. [PubMed: 15870287]
- Basu T, Warne PH, Downward J. Role of Shc in the activation of Ras in response to epidermal growth factor and nerve growth factor. *Oncogene*. 1994; 9:3483–3491. [PubMed: 7970708]
- Carriere C, Young AL, Gunn JR, Longnecker DS, Korc M. Acute pancreatitis markedly accelerates pancreatic cancer progression in mice expressing oncogenic Kras. *Biochem Biophys Res Commun*. 2009
- Castro AF, Rebhun JF, Quilliam LA. Measuring Ras-family GTP levels in vivo—running hot and cold. *Methods*. 2005; 37:190–196. [PubMed: 16289967]
- Collisson EA, Sadanandam A, Olson P, Gibb WJ, Truitt M, Gu S, Cooc J, Weinkle J, Kim GE, Jakkula L, et al. Subtypes of pancreatic ductal adenocarcinoma and their differing responses to therapy. *Nature Med*. 2011; 17:500–503. [PubMed: 21460848]
- De Lisle RC, Logsdon CD. Pancreatic acinar cells in culture: expression of acinar and ductal antigens in a growth-related manner. *Eur J Cell Biol*. 1990; 51:64–75. [PubMed: 2184038]
- Dlugosz AA, Hansen L, Cheng C, Alexander N, Denning MF, Threadgill DW, Magnuson T, Coffey RJ Jr, Yuspa SH. Targeted disruption of the epidermal growth factor receptor impairs growth of squamous papillomas expressing the v-ras(Ha) oncogene but does not block in vitro keratinocyte responses to oncogenic ras. *Cancer Res*. 1997; 57:3180–3188. [PubMed: 9242447]
- Fjallskog ML, Lejonklou MH, Oberg KE, Eriksson BK, Janson ET. Expression of molecular targets for tyrosine kinase receptor antagonists in malignant endocrine pancreatic tumors. *Clin Cancer Res*. 2003; 9:1469–1473. [PubMed: 12684421]
- Friess H, Berberat P, Schilling M, Kunz J, Korc M, Buchler MW. Pancreatic cancer: the potential clinical relevance of alterations in growth factors and their receptors. *J Mol Med*. 1996; 74:35–42. [PubMed: 8834768]

- Gale NW, Kaplan S, Lowenstein EJ, Schlessinger J, Bar-Sagi D. Grb2 mediates the EGF-dependent activation of guanine nucleotide exchange on Ras. *Nature*. 1993; 363:88–92. [PubMed: 8386805]
- Gangarosa LM, Sizemore N, Graves-Deal R, Oldham SM, Der CJ, Coffey RJ. A raf-independent epidermal growth factor receptor autocrine loop is necessary for Ras transformation of rat intestinal epithelial cells. *J Biol Chem*. 1997; 272:18926–18931. [PubMed: 9228072]
- Gidekel Friedlander SY, Chu GC, Snyder EL, Girmius N, Dibelius G, Crowley D, Vasile E, DePinho RA, Jacks T. Context-dependent transformation of adult pancreatic cells by oncogenic K-Ras. *Cancer Cell*. 2009; 16:379–389. [PubMed: 19878870]
- Guerra C, Collado M, Navas C, Schuhmacher AJ, Hernandez-Porras I, Canamero M, Rodriguez-Justo M, Serrano M, Barbacid M. Pancreatitis-induced inflammation contributes to pancreatic cancer by inhibiting oncogene-induced senescence. *Cancer Cell*. 2011; 19:728–739. [PubMed: 21665147]
- Guerra C, Schuhmacher AJ, Canamero M, Grippo PJ, Verdaguier L, Perez-Gallego L, Dubus P, Sandgren EP, Barbacid M. Chronic pancreatitis is essential for induction of pancreatic ductal adenocarcinoma by K-Ras oncogenes in adult mice. *Cancer Cell*. 2007; 11:291–302. [PubMed: 17349585]
- Hansen LA, Woodson RL 2nd, Holbus S, Strain K, Lo YC, Yuspa SH. The epidermal growth factor receptor is required to maintain the proliferative population in the basal compartment of epidermal tumors. *Cancer research*. 2000; 60:3328–3332. [PubMed: 10910032]
- Heid I, Lubeseder-Martellato C, Sipos B, Mazur PK, Lesina M, Schmid RM, Siveke JT. Early requirement of Rac1 in a mouse model of pancreatic cancer. *Gastroenterology*. 2011; 141:719–730. 730 e711–717. [PubMed: 21684285]
- Hingorani SR, Petricoin EF, Maitra A, Rajapakse V, King C, Jacobetz MA, Ross S, Conrads TP, Veenstra TD, Hitt BA, et al. Preinvasive and invasive ductal pancreatic cancer and its early detection in the mouse. *Cancer Cell*. 2003; 4:437–450. [PubMed: 14706336]
- Iverson C, Larson G, Lai C, Yeh LT, Dadson C, Weingarten P, Appleby T, Vo T, Maderna A, Vernier JM, et al. RDEA119/BAY 869766: a potent, selective, allosteric inhibitor of MEK1/2 for the treatment of cancer. *Cancer research*. 2009; 69:6839–6847. [PubMed: 19706763]
- Jaganathan S, Yue P, Turkson J. Enhanced sensitivity of pancreatic cancer cells to concurrent inhibition of aberrant signal transducer and activator of transcription 3 and epidermal growth factor receptor or Src. *J Pharmacol Exp Ther*. 2010; 333:373–381. [PubMed: 20100905]
- Ji B, Tsou L, Wang H, Gaiser S, Chang DZ, Daniluk J, Bi Y, Grote T, Longnecker DS, Logsdon CD. Ras activity levels control the development of pancreatic diseases. *Gastroenterology*. 2009; 137:1072–1082. 1082 e1071–1076. [PubMed: 19501586]
- Jimeno A, Tan AC, Coffa J, Rajeshkumar NV, Kulesza P, Rubio-Viqueira B, Wheelhouse J, Diosdado B, Messersmith WA, Iacobuzio-Donahue C, et al. Coordinated epidermal growth factor receptor pathway gene overexpression predicts epidermal growth factor receptor inhibitor sensitivity in pancreatic cancer. *Cancer research*. 2008; 68:2841–2849. [PubMed: 18413752]
- Kawaguchi Y, Cooper B, Gannon M, Ray M, MacDonald RJ, Wright CV. The role of the transcriptional regulator Ptf1a in converting intestinal to pancreatic progenitors. *Nat Genet*. 2002; 32:128–134. [PubMed: 12185368]
- Kobrin MS, Funatomi H, Friess H, Buchler MW, Stathis P, Korc M. Induction and expression of heparin-binding EGF-like growth factor in human pancreatic cancer. *Biochem Biophys Res Commun*. 1994; 202:1705–1709. [PubMed: 8060360]
- Korc M, Friess H, Yamanaka Y, Kobrin MS, Buchler M, Beger HG. Chronic pancreatitis is associated with increased concentrations of epidermal growth factor receptor, transforming growth factor alpha, and phospholipase C gamma. *Gut*. 1994; 35:1468–1473. [PubMed: 7959207]
- Larbouret C, Robert B, Navarro-Teulon I, Thezenas S, Ladjemi MZ, Morisseau S, Campigna E, Bibeau F, Mach JP, Pelegrin A, Azria D. In vivo therapeutic synergism of anti-epidermal growth factor receptor and anti-HER2 monoclonal antibodies against pancreatic carcinomas. *Clin Cancer Res*. 2007; 13:3356–3362. [PubMed: 17545543]
- Lee KE, Bar-Sagi D. Oncogenic KRas suppresses inflammation-associated senescence of pancreatic ductal cells. *Cancer Cell*. 2010; 18:448–458. [PubMed: 21075310]
- Lee TC, Threadgill DW. Generation and validation of mice carrying a conditional allele of the epidermal growth factor receptor. *Genesis*. 2009; 47:85–92. [PubMed: 19115345]

- Luttges J, Reinecke-Luthge A, Mollmann B, Menke MA, Clemens A, Klimpfinger M, Sipos B, Kloppel G. Duct changes and K-ras mutations in the disease-free pancreas: analysis of type, age relation and spatial distribution. *Virchows Arch.* 1999; 435:461–468. [PubMed: 10592048]
- Marino S, Vooijs M, van Der Gulden H, Jonkers J, Berns A. Induction of medulloblastomas in p53-null mutant mice by somatic inactivation of Rb in the external granular layer cells of the cerebellum. *Genes Dev.* 2000; 14:994–1004. [PubMed: 10783170]
- Mascia F, Cataisson C, Lee TC, Threadgill D, Mariani V, Amerio P, Chandrasekhara C, Souto Adeva G, Girolomoni G, Yuspa SH, Pastore S. EGFR regulates the expression of keratinocyte-derived granulocyte/macrophage colony-stimulating factor in vitro and in vivo. *The Journal of investigative dermatology.* 2010; 130:682–693. [PubMed: 19890352]
- Means AL, Meszoely IM, Suzuki K, Miyamoto Y, Rustgi AK, Coffey RJ Jr, Wright CV, Stoffers DA, Leach SD. Pancreatic epithelial plasticity mediated by acinar cell transdifferentiation and generation of nestin-positive intermediates. *Development.* 2005; 132:3767–3776. [PubMed: 16020518]
- Means AL, Ray KC, Singh AB, Washington MK, Whitehead RH, Harris RC Jr, Wright CV, Coffey RJ Jr, Leach SD. Overexpression of heparin-binding EGF-like growth factor in mouse pancreas results in fibrosis and epithelial metaplasia. *Gastroenterology.* 2003; 124:1020–1036. [PubMed: 12671899]
- Miyamoto Y, Maitra A, Ghosh B, Zechner U, Argani P, Iacobuzio-Donahue CA, Sriuranpong V, Iso T, Meszoely IM, Wolfe MS, et al. Notch mediates TGF alpha-induced changes in epithelial differentiation during pancreatic tumorigenesis. *Cancer Cell.* 2003; 3:565–576. [PubMed: 12842085]
- Monick MM, Cameron K, Staber J, Powers LS, Yarovinsky TO, Koland JG, Hunninghake GW. Activation of the epidermal growth factor receptor by respiratory syncytial virus results in increased inflammation and delayed apoptosis. *J Biol Chem.* 2005; 280:2147–2158. [PubMed: 15542601]
- Moore MJ, Goldstein D, Hamm J, Figier A, Hecht JR, Gallinger S, Au HJ, Murawa P, Walde D, Wolff RA, et al. Erlotinib plus gemcitabine compared with gemcitabine alone in patients with advanced pancreatic cancer: a phase III trial of the National Cancer Institute of Canada Clinical Trials Group. *J Clin Oncol.* 2007; 25:1960–1966. [PubMed: 17452677]
- Morris, JPT; Cano, DA.; Sekine, S.; Wang, SC.; Hebrok, M. Beta-catenin blocks Kras-dependent reprogramming of acini into pancreatic cancer precursor lesions in mice. *J Clin Invest.* 2010; 120:508–520. [PubMed: 20071774]
- Natarajan A, Wagner B, Sibilina M. The EGF receptor is required for efficient liver regeneration. *Proc Natl Acad Sci U S A.* 2007; 104:17081–17086. [PubMed: 17940036]
- Normanno N, De Luca A, Bianco C, Strizzi L, Mancino M, Maiello MR, Carotenuto A, De Feo G, Caponigro F, Salomon DS. Epidermal growth factor receptor (EGFR) signaling in cancer. *Gene.* 2006; 366:2–16. [PubMed: 16377102]
- Pino MS, Shrader M, Baker CH, Cognetti F, Xiong HQ, Abbruzzese JL, McConkey DJ. Transforming growth factor alpha expression drives constitutive epidermal growth factor receptor pathway activation and sensitivity to gefitinib (Iressa) in human pancreatic cancer cell lines. *Cancer research.* 2006; 66:3802–3812. [PubMed: 16585207]
- Ringel J, Jesnowski R, Moniaux N, Luttges J, Ringel J, Choudhury A, Batra SK, Kloppel G, Lohr M. Aberrant expression of a disintegrin and metalloproteinase 17/tumor necrosis factor-alpha converting enzyme increases the malignant potential in human pancreatic ductal adenocarcinoma. *Cancer Res.* 2006; 66:9045–9053. [PubMed: 16982746]
- Sahin U, Weskamp G, Kelly K, Zhou HM, Higashiyama S, Peschon J, Hartmann D, Saftig P, Blobel CP. Distinct roles for ADAM10 and ADAM17 in ectodomain shedding of six EGFR ligands. *J Cell Biol.* 2004; 164:769–779. [PubMed: 14993236]
- Sandgren EP, Luetke NC, Palmiter RD, Brinster RL, Lee DC. Overexpression of TGF alpha in transgenic mice: induction of epithelial hyperplasia, pancreatic metaplasia, and carcinoma of the breast. *Cell.* 1990; 61:1121–1135. [PubMed: 1693546]
- Sharma A, Zangen DH, Reitz P, Taneja M, Lissauer ME, Miller CP, Weir GC, Habener JF, Bonner-Weir S. The homeodomain protein IDX-1 increases after an early burst of proliferation during pancreatic regeneration. *Diabetes.* 1999; 48:507–513. [PubMed: 10078550]

- Sibilia M, Fleischmann A, Behrens A, Stingl L, Carroll J, Watt FM, Schlessinger J, Wagner EF. The EGF receptor provides an essential survival signal for SOS-dependent skin tumor development. *Cell*. 2000; 102:211–220. [PubMed: 10943841]
- Singh AB, Harris RC. Autocrine, paracrine and juxtacrine signaling by EGFR ligands. *Cellular signalling*. 2005; 17:1183–1193. [PubMed: 15982853]
- Siveke JT, Einwachter H, Sipos B, Lubeseder-Martellato C, Kloppel G, Schmid RM. Concomitant pancreatic activation of Kras(G12D) and Tgfa results in cystic papillary neoplasms reminiscent of human IPMN. *Cancer Cell*. 2007; 12:266–279. [PubMed: 17785207]
- Strobel O, Dor Y, Alsina J, Stirman A, Lauwers G, Trainor A, Castillo CF, Warshaw AL, Thayer SP. In vivo lineage tracing defines the role of acinar-to-ductal transdifferentiation in inflammatory ductal metaplasia. *Gastroenterology*. 2007; 133:1999–2009. [PubMed: 18054571]
- Tang J, Zarbock A, Gomez I, Wilson CL, Lefort CT, Stadtmann A, Bell B, Huang LC, Ley K, Raines EW. Adam17-dependent shedding limits early neutrophil influx but does not alter early monocyte recruitment to inflammatory sites. *Blood*. 2011; 118:786–794. [PubMed: 21628404]
- Tobita K, Kijima H, Dowaki S, Kashiwagi H, Ohtani Y, Oida Y, Yamazaki H, Nakamura M, Ueyama Y, Tanaka M, et al. Epidermal growth factor receptor expression in human pancreatic cancer: Significance for liver metastasis. *Int J Mol Med*. 2003; 11:305–309. [PubMed: 12579331]
- Zhao S, Wang Y, Cao L, Ouellette MM, Freeman JW. Expression of oncogenic K-ras and loss of Smad4 cooperate to induce the expression of EGFR and to promote invasion of immortalized human pancreas ductal cells. *Int J Cancer*. 2010; 127:2076–2087. [PubMed: 20473902]
- Zhu Z, Kleeff J, Friess H, Wang L, Zimmermann A, Yarden Y, Buchler MW, Korc M. Epiregulin is Up-regulated in pancreatic cancer and stimulates pancreatic cancer cell growth. *Biochem Biophys Res Commun*. 2000; 273:1019–1024. [PubMed: 10891365]

HIGHLIGHTS

KRAS-mediated tumorigenesis is inhibited in pancreatic *Egfr* and *Adam17* knockouts

Pancreatitis-induced tumors are blocked by pancreatic *Egfr* or *Adam17* ablation

Pancreatic *Egfr* and *Adam17* knockouts resist metaplasia *in vitro* and *in vivo*

KRAS requires EGFR to robustly activate ERK, which is necessary for tumorigenesis

SIGNIFICANCE

The almost universal lethality of PDA has led to the intense study of genetic mutations responsible for its formation and progression. The most common oncogenic mutations associated with all PDA stages are found in the *KRAS* gene, suggesting it as the primary initiator of pancreatic neoplasia. However, mutant *Kras* expression throughout the mouse pancreatic parenchyma shows that the oncogene remains largely indolent until secondary events, such as pancreatitis, unlock its transforming potential. We find KRAS requires an inside-outside-in signaling axis that involves ligand-dependent EGFR activation to initiate the signal transduction and cell biological changes that link PDA and pancreatitis.

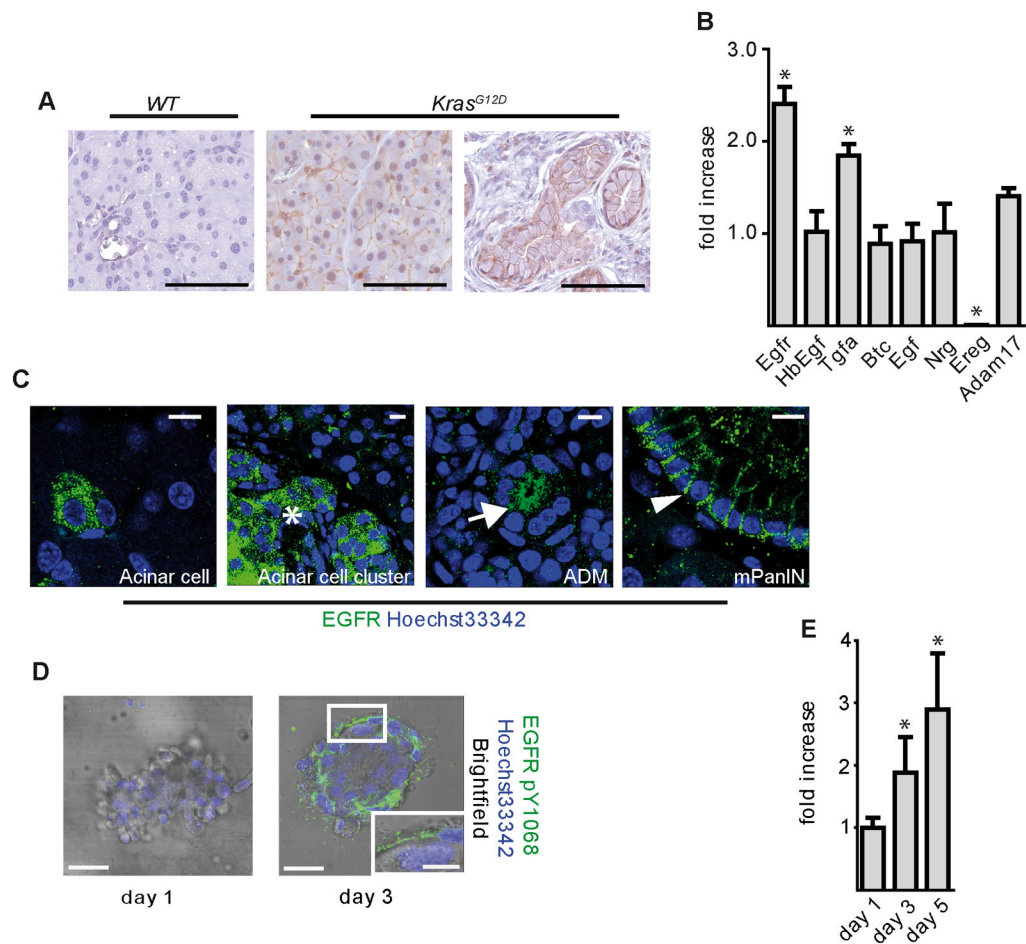


Figure 1. EGFR signaling during mPanIN development

(A) IHC for EGFR pY1068 in wild-type and *Kras^{G12D}* pancreata. Scale bars = 50 μ m. (B) qRT-PCR analysis for *Egfr*, its ligands and *Adam17*. Error bars are \pm SEM. (n = 3, * p < 0.05). (C) Confocal IF staining for total EGFR in distinct single acinar cells, acinar cell clusters (*), ADM (arrow), and mPanINs (arrowhead) of *Kras^{G12D}* pancreata. Scale bars = 10 μ m. (D) IF for EGFR pY1068 and (E) qRT-PCR analysis of *Egfr* in *Kras^{G12D}* acinar cell explants. Scale bars = 10 μ m for micrographs, 50 μ m for inset. Error bars are \pm SEM (n = 3, * p < 0.05). See also Figure S1.

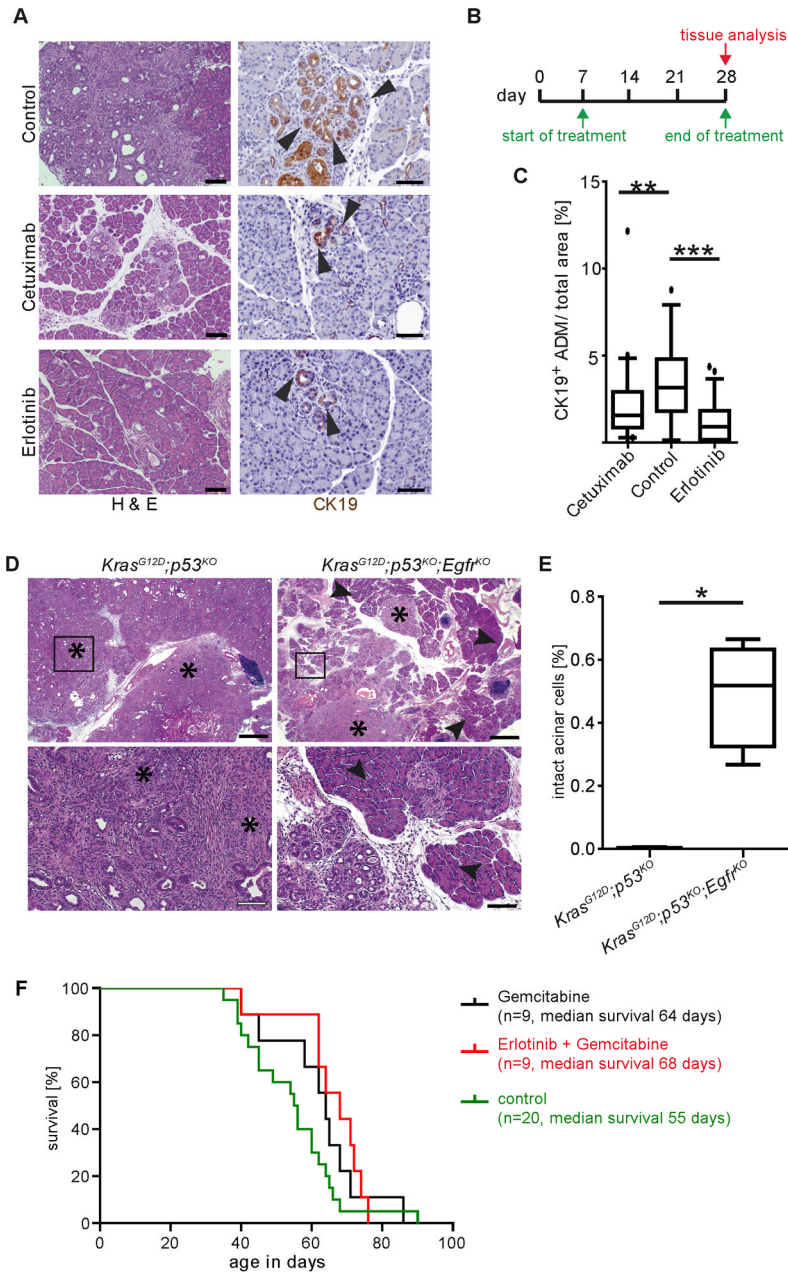


Figure 2. Inhibition of EGFR signaling blocks KRAS-driven tumorigenesis but not PDA progression

(A) H&E and CK19 IHC of 4 week old *Kras^{G12D};p53^{KO}* control, cetuximab and erlotinib treated pancreata. Arrowheads indicate CK19⁺ structures. Scale bars = 100 μ m for H&E and 50 μ m for CK19 panels. (B) Schematic of cetuximab and erlotinib treatment protocols. (C) Quantitation of CK19⁺ structures (n = 3, ** p < 0.01, *** p < 0.001). (D) Histology of 9 week old *Kras^{G12D};p53^{KO}* and *Kras^{G12D};p53^{KO};Egfr^{KO}* pancreata. Asterisks indicate areas of invasive PDA. Arrowheads highlight areas of normal acinar tissue. Scale bars, upper panels = 200 μ m, lower panels = 50 μ m. (E) Quantitation of normal acinar area in *Kras^{G12D};p53^{KO}* and *Kras^{G12D};p53^{KO};Egfr^{KO}* pancreata. (F) Kaplan-Meier curve depicting survival of *Kras^{G12D};p53^{KO}* mice treated with gemcitabine or erlotinib plus gemcitabine after progression to PDA. See also Figure S2.

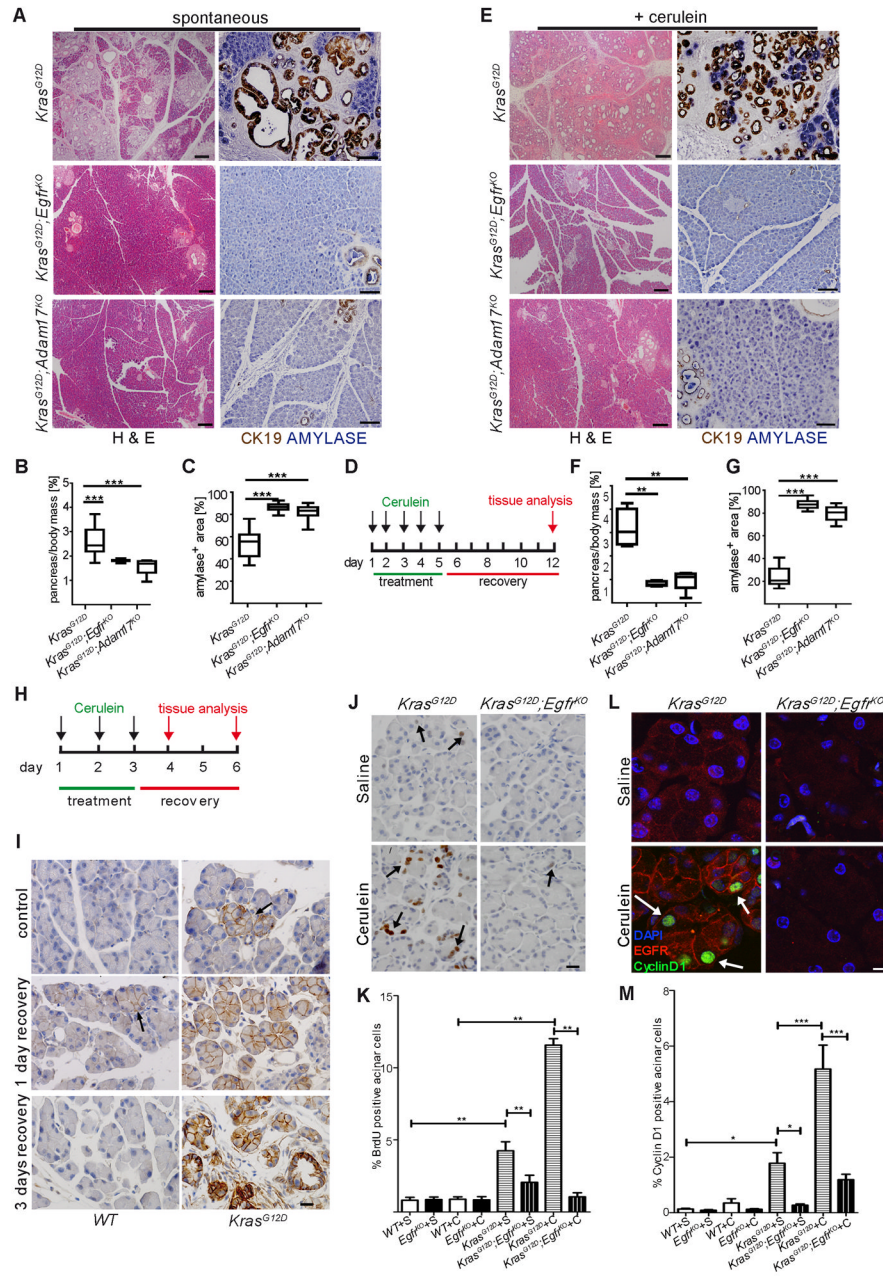


Figure 3. Genetic ablation of EGFR activity prevents KRAS-driven PDA development (A–C) Spontaneous and (D–G) cerulein-induced mPanIN formation in *Kras*^{G12D};*Egfr*^{KO} and *Kras*^{G12D};*Adam1*^{7KO} mice compared to *Kras*^{G12D} controls, shown by H&E (left panels, scale bars = 200 μ m) and dual IHC for CK19 (brown) and amylase (blue) (right panels, scale bars = 100 μ m). Quantitation of pancreas-to-body weight ratios (B&F) and amylase positive area (C&G) ($n > 6$, ** $p < 0.01$, *** $p < 0.001$) compared to control. (H) Truncated cerulein treatment protocol for analysis of premetaplastic signaling. (I) EGFR IHC in saline-treated (control) and cerulein treated WT (left panels) and *Kras*^{G12D} (right panels) pancreata with 1 day and 3 days recovery. Arrows indicate focal areas of high EGFR expression. $n = 3$, scale bars = 20 μ m. (J) BrdU incorporation measured by IHC in acinar cells of saline or cerulein-treated *Kras*^{G12D} and *Kras*^{G12D};*Egfr*^{KO} pancreata with 3 days recovery. Arrows indicate positive acinar nuclei. Scale bar = 20 μ m (K) Counts of BrdU⁺ acinar cells, $n=3$,

** $p < 0.01$. (L) Co-IF for CyclinD1 (green) and EGFR (red) in saline or cerulein-treated *Kras^{G12D}* and *Kras^{G12D};Egfr^{KO}*. Arrows indicate some positive acinar nuclei. Scale bar = 10 μm (M) Quantitation of CyclinD1 expression (* $p < 0.05$, *** $p < 0.001$, all other differences were not significant. $n=3$). Error bars in all panels are \pm SEM. See also Figure S3.

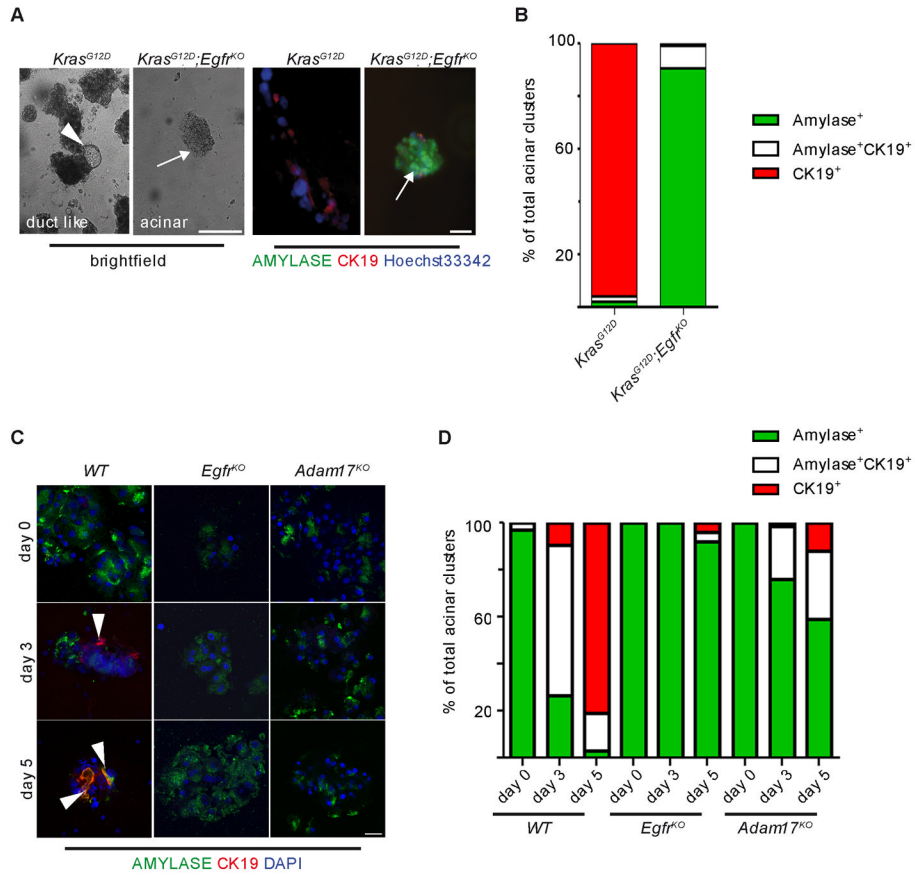


Figure 4. EGFR signaling is required for acinar transdifferentiation in three dimensional primary culture

(A) Light microscopy (left panels) and co-IF for amylase (green) and CK19 (red, right panels) in *Kras^{G12D}* and *Kras^{G12D};Egfr^{KO}* acinar cell explants after three days in three-dimensional collagen culture. Arrowhead indicates area of ductal morphology in *Kras^{G12D}* explants, compared to maintained acinar cell morphology and amylase expression in *Kras^{G12D};Egfr^{KO}* explants (arrows). Scale bars = 20 μ m. (B) Quantitation of amylase and CK19 positive acinar clusters on day 3 of culture. (C) Co-IF for amylase (green) and CK19 (red) in cerulein-treated WT (left panels) *Egfr^{KO}* (middle panels) and *Adam17^{KO}* acinar cell explants (right panels). Arrowheads indicate CK19⁺ cells, scale bars = 20 μ m. (D) Quantitation of amylase and CK19 positive acinar clusters in cerulein-treated explant cultures. See also Figure S4.

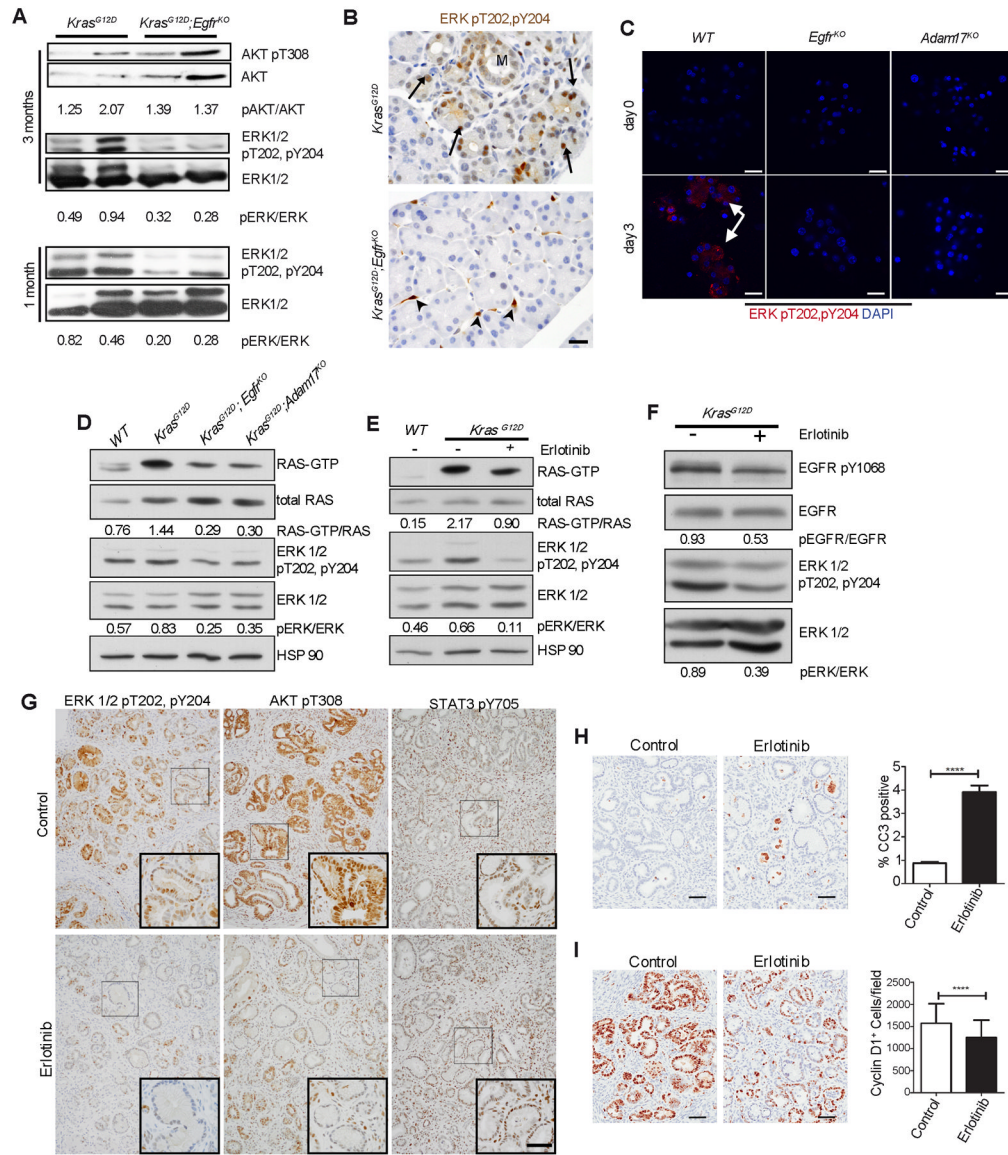


Figure 5. Endogenous EGFR is required for robust activation of RAS and ERK

(A) Western blot analysis of whole pancreatic lysates for active pAKT and pERK in *Kras^{G12D}* and *Kras^{G12D};Egfr^{KO}* mice, at 3 months (upper and middle panels) and pERK at 1 month of age (lower panels). Numbers indicate densitometric quantitation of pERK/total ERK and pAKT/AKT ratios, of representative blots shown. $n=4$. (B) IHC for active pERK in 6 week old *Kras^{G12D}* and *Kras^{G12D};Egfr^{KO}* pancreata. Arrows indicate areas of focal acinar cell staining. Metaplasia is indicated (M). Arrowheads indicate stromal cell staining. Micrographs are representative of 6 mice. Scale bar = 20 μm . (C) IF staining for active pERK in acinar cell explants of cerulein treated wild-type (WT), *Egfr^{KO}* and *Adam17^{KO}* explants at 0 and 3 days of culture. Arrows indicate areas of positive staining. Scale bar = 20 μm . (D) Active RAS pull-down assays from lysates of isolated primary acinar cells from wild-type (WT), *Kras^{G12D}*, *Kras^{G12D};Egfr^{KO}* and *Kras^{G12D};Adam17^{KO}* mice. Numbers indicate densitometric quantitation of the ratio of GTP-bound and total RAS of representative blots shown. Western blots show concomitant relative ERK activity (pERK/ERK) in these lysates. $n=3$. (E) GTP-bound RAS/total RAS and pERK/total ERK ratios in

isolated acinar cells treated with erlotinib for 6 hours. Numbers indicate quantitation of representative blots shown. n=3. (F) *Kras*^{G12D} mice were cerulein-treated as in Figure 3D to induce uniform tumorigenesis, then treated with vehicle or 100 mg/kg erlotinib 12, 6 and 2 hours before sacrifice. Shown are western blots of pY1068 and total EGFR and pERK and total ERK. Numbers indicate ratios of representative blots shown. n=3. (G) IHC for active pERK, pAKT and pSTAT3 in vehicle or erlotinib treated mice described in (F). Scale bar = 100µm for primary micrographs, 50µm for insets. (H&I) IHC and quantitation for cleaved caspase-3 (CC3, H) and CyclinD1 (I) in vehicle or erlotinib treated mice described in (F). Scale bars = 50µm. Error bars are +/- SEM. See also Figure S5.

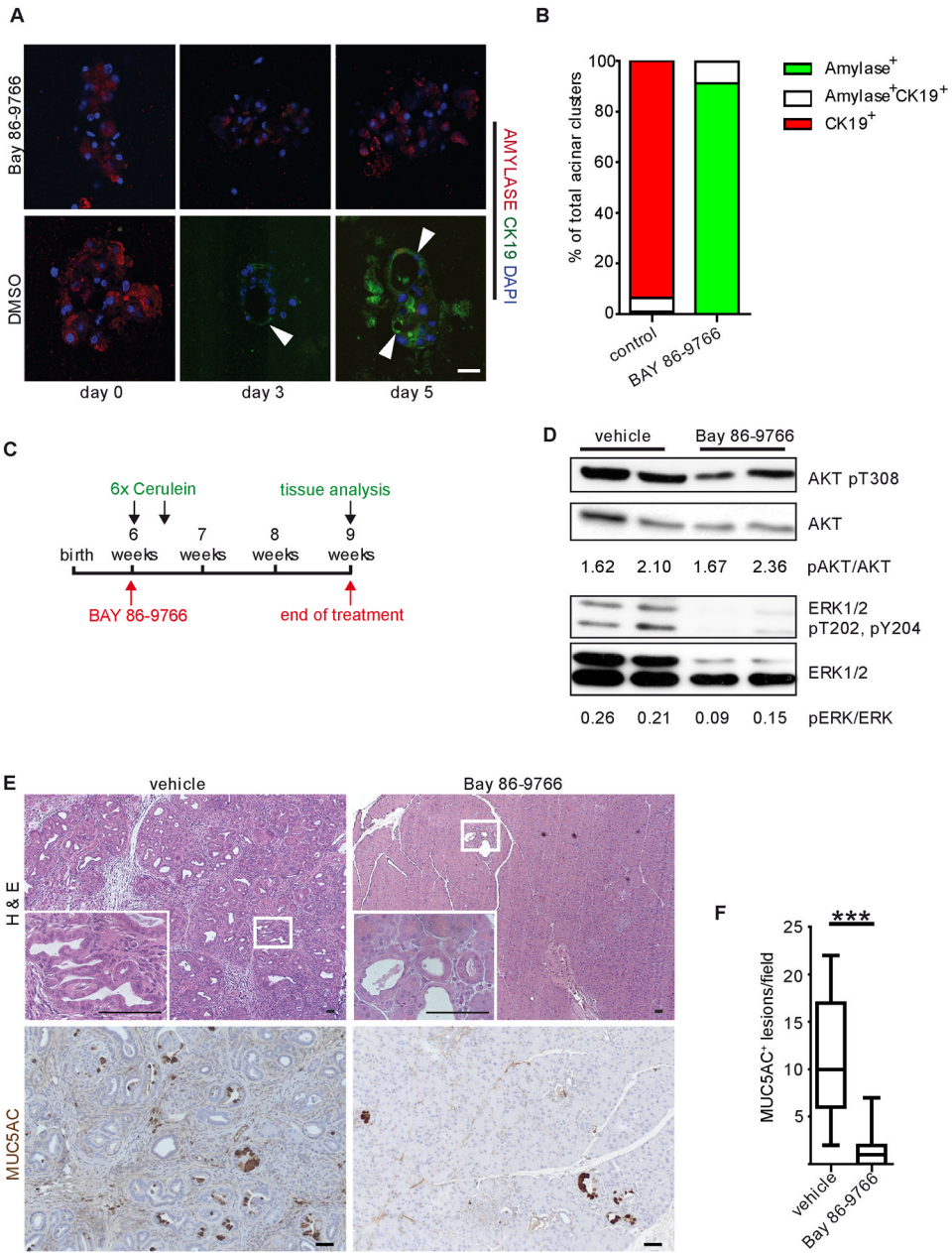


Figure 6. ERK activity is critical for metaplasia and neoplasia

(A) Co-IF for amylase and CK19 in acinar cell explants of *Kras*^{G12D} mice treated with either the MEK inhibitor BAY 86-9766 or vehicle. Arrowheads point to CK19⁺ duct-like structures. Scale bar = 20 μm. (B) Quantitation of amylase⁺ and CK19⁺ cell clusters is representative of at least 3 independent experiments per treatment. (C) Schematic illustration of pancreatitis induction in *Kras*^{G12D} mice with a BAY 86-9766 treatment regimen. In 6 week old *Kras*^{G12D} mice pancreatitis was induced by 6 hourly injections with 50 μg/kg cerulein on two consecutive days. Mice were treated either with a daily oral dose of BAY 86-9766 or vehicle, 6 days per week for 3 consecutive weeks, beginning on the first day of cerulein treatment. (D) Western blot analysis for active pERK and pAKT in control and BAY 86-9766 treated mice. Numbers indicate quantitation of ratios of blots shown, as indicated. (E) Histological analysis and IHC for the PanIN marker MUC5AC in vehicle and

BAY 86-9766 treated mice (inset, n = 3). Scale bars = 50 μm . (F) Quantitation of MUC5AC⁺ lesions in BAY 86-9766 treated mice compared to controls (***) p < 0.001).